Porous Silica Materials Derivatized with Cu and Ag Cations for Selective Propene−Propane Adsorption from the Gas Phase: Aluminosilicate Ion-Exchanged Monoliths

M. Kargol,[†,§] J. Zajac,*[,†] D. J. Jones,[†] Th. Steriotis,[‡] J. Rozière,[†] and P. Vitse[†]

Laboratoire des Agrégats Moléculaires et Matériaux Inorganiques, UMR 5072, Université Montpellier 2, Place E. Bataillon, 34095 Montpellier Cedex 5, France, and Institute of Physical Chemistry, National Center for Scientific Research "DEMOKRITOS", Aghia Paraskevi, 153-10, Athens, Greece

Received March 30, 2004. Revised Manuscript Received July 14, 2004

Copper- and silver-derivatized aluminosilicate materials possessing uniformly sized mesopores have been synthesized and tested for selective separation of gaseous propene/propane mixtures. Small monoliths of cylindrical shape were prepared via the direct liquid crystal templating (DLCT) pathway using commercially available nonionic surfactants as templates. Calcined samples prepared with Si:Al ratios of 20, 10, and 5 were characterized by powder X-ray diffraction and ^{27}Al magic-angle spinning NMR. The shaped aluminosilicates were subsequently functionalized with Cu(II) and Ag(I) by ion exchange from 0.5 mol L^{-1} $Cu(NO_3)_2$ and 1 mol L^{-1} $AgNO_3$ aqueous solutions. The overall Cu or Ag contents in the resulting samples were quantified by atomic absorption spectroscopy. Estimates of the BET specific surface area and porous structure parameters were based on nitrogen gas adsorption at 77 K. The ion-exchange procedure was found to lead to monolithic materials possessing larger pores and lower specific surface areas compared to the pristine samples. A Cu(I)-derivatized sample was obtained by partial reduction of a Cu(II)-exchanged precursor. Individual adsorption of propene and propane onto derivatized shaped materials was studied under static conditions at room temperature, and the ideal propene/propane selectivity coefficient was calculated as a function of the molar fraction of propene in the binary gas mixture. The selectivity of all samples to propene exhibited a downward trend with increasing propene molar fraction. The nature and the number of surface metal sites were shown to be crucial for selective adsorption of propene against propane, monovalent cationic sites being the most appropriate for this purpose.

Introduction

Low-molecular-weight unsaturated hydrocarbons, and propene in particular, are very important chemicals for use in the petrochemical industry. The main source of such alkenes is large-scale selective separation from their saturated counterparts in the liquefied petroleum gas mixture issued from fluid catalytic cracking. The separation procedure is currently distillation, which is considered as one of the most energy-consuming industrial processes due to the very close relative volatilities of alkenes and corresponding alkanes and the cryogenic temperature conditions required.[1] In this context, numerous membrane and adsorption technologies have already been proposed as cost-efficient alternatives for alkene/alkane separation,[2−12] while only a few reports are devoted to separation by selective adsorption onto solid substrates, such as carbon black,[11] zeolite 13X,[12] activated carbon, silica gel and zeolite A,[13] or ordered mesoporous silica.[14,15] The most promising technological approach is based on the mechanism of π-complexation between the alkene double bond and transition metal cations, mostly Cu or Ag.

The idea of exploiting π-complexation dates from the studies made on specific interactions of alkenes with solid cuprous halides reported by Gilliland et al.[16,17]

* Corresponding author. E-mail: zajac@univ-montp2.fr.
† Université Montpellier 2.
‡ National Center for Scientific Research "DEMOKRITOS".
§ Permanent address: Institute of Chemical Engineering, Polish Academy of Sciences, Baltycka 5, 44-100 Gliwice, Poland.

(1) Eldridge, R. B. *Ind. Eng. Chem. Res.* **1993**, *32*, 2208.
(2) Staudt-Bickel, C.; Koros, W. J. *J. Membr. Sci.* **2000**, *170*, 205.
(3) Hsiue, G.-H.; Yang, J.-S. *J. Membr. Sci.* **1993**, *82*, 117.
(4) Yang, J.-S.; Hsiue, G.-H. *J. Membr. Sci.* **1998**, *138*, 203.
(5) Teramoto, M.; Takeuchi, N.; Maki, T.; Matsuyama, H. *Sep. Purif. Technol.* **2002**, *28*, 117.
(6) Sungpet, A.; Way, J. D.; Koval, C. A.; Eberhart, M. E. *J. Membr. Sci.* **2001**, *189*, 271.
(7) Chang, J.-W.; Marrero, T. R.; Yasuda, H. K. *J. Membr. Sci.* **2002**, *205*, 91.
(8) LeBlanc, O. H., Jr.; Ward, W. J.; Matson, S. L.; Kimura, S. G. *J. Membr. Sci.* **1980**, *6*, 339.
(9) Ho, W. S.; Dalrymple, D. C. *J. Membr. Sci.* **1994**, *91*, 13.
(10) Pinnau, I.; Toyl, L. G. *J. Membr. Sci.* **2001**, *184*, 39.
(11) Glanz, P.; Körner, B.; Findenegg, G. H. *Adsorpt. Sci. Technol.* **1984**, *1*, 41.
(12) Shue, C. M.; Kulvaranon, S.; Findlay, M. E.; Liapis, A. I. *Sep. Technol.* **1990**, *1*, 18.
(13) Järvelin, H.; Fair, J. R. *Ind. Eng. Chem. Res.* **1993**, *32*, 2201.
(14) Newalkar, B. L.; Choudary, N. V.; Kumar, P.; Komarneni, S.; Bhat, S. G. T. *Chem. Mater.* **2002**, *14*, 304.
(15) Newalkar, B. L.; Choudary, N. V.; Turaga, U. T.; Vijayalakshimi, R. P.; Kumar, P.; Komarneni, S.; Bhat, S. G. T. *Chem. Mater.* **2003**, *15*, 1474.

10.1021/cm040051l CCC: $27.50
Published on Web 08/31/2004

Preferential sorption of the alkene via the formation of π-complexes has been shown to result from charge donor−acceptor interactions between the appropriate atomic and molecular orbitals. Charge donation takes place from the π molecular orbitals of the alkene to the empty atomic orbitals of the transition metal, while back-donation of charge occurs from the d-type atomic orbitals of the metal to the empty antibonding orbitals of the alkene. In consequence, the bonding of the alkene to the metal cation is significantly stronger than the van der Waals interaction underlying simple physisorption. On the other hand, π-complexation is weaker than the usual ligand coordination and the chemically unchanged alkene molecule may be easily desorbed by increasing the temperature or decreasing the pressure in the system.

Within the framework of membrane technology, π-complexation facilitated transport membranes have been developed during the past decade.[3−6] These are polymer membranes in which a Ag salt is employed as a carrier to selectively complex with the alkene component of the feed gas. They are highly alkene/alkane selective and have adequate alkene permeabilities. Nevertheless, some important disadvantages, related to their poor mechanical and chemical stability and particular process requirements necessary to provide mobility for the alkene-selective carrier,[7−9] make them less useful for commercial applications. Solid polymer electrolyte membranes have found novel application in selective alkene/alkane separation. $AgBF_4$-loaded, rubbery, or polyether-based membranes have good selectivity characteristics.[10] In the case of adsorptive separation, porous solids possessing high specific areas have been used as substrates and novel cation−substrate combinations have been developed and tested. These include Ag salts on anion-exchange resins,[17,18] Ag-exchanged resins,[19−21] monolayer $CuCl/\gamma$-Al_2O_3,[20] monolayer CuCl on pillared clays,[22,23] monolayer $AgNO_3/SiO_2$,[24] γ-Al_2O_3, SiO_2, and MCM-41 $AgNO_3$ impregnated by incipient wetness,[25] as well as AgY[25] and CuY[26] zeolites.

To ensure the economic viability of the separation process, membranes or solid adsorbents should exhibit appropriate fluid transport behavior, adsorption capacity, reversibility, and regeneration ability. There is thus considerable scope in searching for materials which meet these requirements. For the purpose of the present work, novel Cu- and Ag-derivatized aluminosilicate monoliths possessing uniformly sized small mesopores have been prepared and their propene/propane sorption properties have been characterized. The synthesis route described here offers an opportunity of obtaining selective adsorbents with desired shape and size without any further treatment, thereby obviating the necessity to press or extrude the pristine powdered material into an ultimate form suitable for industrial use. Monoliths derivatized with Ag and Cu cations have been obtained by ion exchange and their properties are compared with those of pristine samples.

Experimental Section

Chemicals. The polyoxyethylenated nonionic surfactant, Brij 30, and tetraethyl orthosilicate, TEOS, were obtained from Aldrich, aluminum nitrate, $Al(NO_3)_3 \cdot 9H_2O$, and copper nitrate, $Cu(NO_3)_2 \cdot 3H_2O$, were purchased from Merck. Silver nitrate, $AgNO_3$, and a 0.1 M nitric acid solution, used to adjust the pH of the aqueous phase, were Fisher products. Gaseous ammonia, nitrogen, propane, and propene of high purity were supplied by Air Liquide.

Synthesis. Macroscopic nanostructured monoliths were synthesized via the direct liquid crystal templating (DLCT) pathway in high-concentration amphiphilic solutions.[27]

In a typical synthesis, acidified solution of surfactant was mixed with TEOS under constant stirring at room temperature. The mass ratio of water:surfactant:TEOS was 1:1:3. $Al(NO_3)_3 \cdot 9H_2O$ was added to the solution of the surfactant in TEOS to obtain Si:Al molar ratios of 20, 10, and 5 in the resulting materials. These aluminosilicates are designated as SiAl20, SiAl10, and SiAl5, respectively. The homogeneous transparent mixture was placed under vacuum for at least 2 h in order to remove ethanol produced during the synthesis and then was kept at a constant temperature of 60 °C to give a viscous liquid. This viscous liquid was poured into appropriate cylindrical moulds (length: 10 cm, internal diameter: 2 mm) and aged for several days, first at room temperature and then at 40 or 60 °C. The resulting aluminosilicate cylinders were calcined at 560 °C for 6 h under a flow of air.

Some monolithic samples were subsequently functionalized with copper and silver by ion exchange in an aqueous medium. The dried sample was first stored above ammonium hydroxide for 2 h and then put into contact with 0.5 mol L^{-1} $Cu(NO_3)_2$ and 1 mol L^{-1} $AgNO_3$ aqueous solutions. The ion exchange was carried out at room temperature for 24 h under constant shaking, and then the sample was removed from the supernatant, rinsed with water, and dried.

Characterization. The XRD patterns of calcined samples were recorded using Philips X'Pert diffractometer with Cu Kα radiation. Solid state ^{27}Al NMR spectra were recorded at 104.3 MHz using a Bruker ASX400 spectrometer. For a Cu-exchanged monolith, the surface reduction of Cu(II) into Cu(I) and then into metallic Cu was investigated by temperature-programmed reduction (TPR) using a Micromeritics AutoChem 2910 Analyzer. The TPR experiments were carried out in the temperature range from −50 to 800 °C (heating rate 2 °C min^{-1}) under a flow of H_2. To determine the ion-exchange capacity of aluminosilicates monoliths, solid samples were first loaded with Cu(II) or Ag(I) from aqueous solutions of $Cu(NO_3)_2$ or $AgNO_3$, then rinsed with water, and dried. Small portions (about 50 mg) of given samples were dissolved in 4 mL of a concentrated HF solution and diluted with distilled water. The resulting clear solutions were analyzed for Cu and Ag concentrations by atomic absorption spectroscopy (AAS) using a PYE UNICAM SP9 spectrometer equipped with a hollow cathode lamp at a wavelength of 324.8 nm for copper and 328.1 nm for silver.

Gas Adsorption Measurements. The surface area and pore structure parameters of cylindrical samples were evaluated from nitrogen adsorption−desorption measurements carried out using an automated volumetric Analsorb 9011 apparatus. Adsorption/desorption isotherms were measured at 77

(16) Gilliland, E. R.; Seebold, J. E.; FitzHugh, J. R.; Morgan, P. S. *J. Am. Chem. Soc.* **1939**, *61*, 1960.
(17) Gilliland, E. R.; Bliss, H. L.; Kip, C. E. *J. Am. Chem. Soc.* **1941**, *63*, 2088.
(18) Hirai, H.; Hara, S.; Komiyama, M. *Angew. Macromol. Chem.* **1985**, *130*, 207.
(19) Hirai, H.; Kurima, K.; Wada, K.; Komiyama, M. *Chem. Lett.* **1985**, 1513.
(20) Yang, R. T.; Kikkinides, E. S. *AIChE J.* **1995**, *41*, 509.
(21) Wu, Z.; Han, S. S.; Cho, S. H.; Kim, J. N.; Chue, K. T.; Yang, R. T. *Ind. Eng. Chem. Res.* **1997**, *36*, 2749.
(22) Cheng, L. S.; Yang, R. T. *Adsorption* **1995**, *1*, 61.
(23) Choudary, N. V.; Kumar, P.; Bhat, T. S. G.; Cho, S. H.; Han, S. S.; Kim, J. N. *Ind. Eng. Chem. Res.* **2002**, *41*, 2728.
(24) Rege, S. U.; Padin, J.; Yang, R. T. *AIChE J.* **1998**, *44*, 799.
(25) Padin, J.; Yang, R. T. *Chem. Eng. Sci.* **2000**, *55*, 2607.
(26) Cen, P. L. In *Separation and Purification Technology*; Li, N. N., Calo, J. M., Eds.; Marcel Dekker: New York, 1992.
(27) Rozière, J.; Brandhorst, M.; Dutartre, R.; Jacquin, M.; Jones, D. J.; Vitse, P.; Zajac, J. *J. Mater. Chem.* **2001**, *11*, 3254.

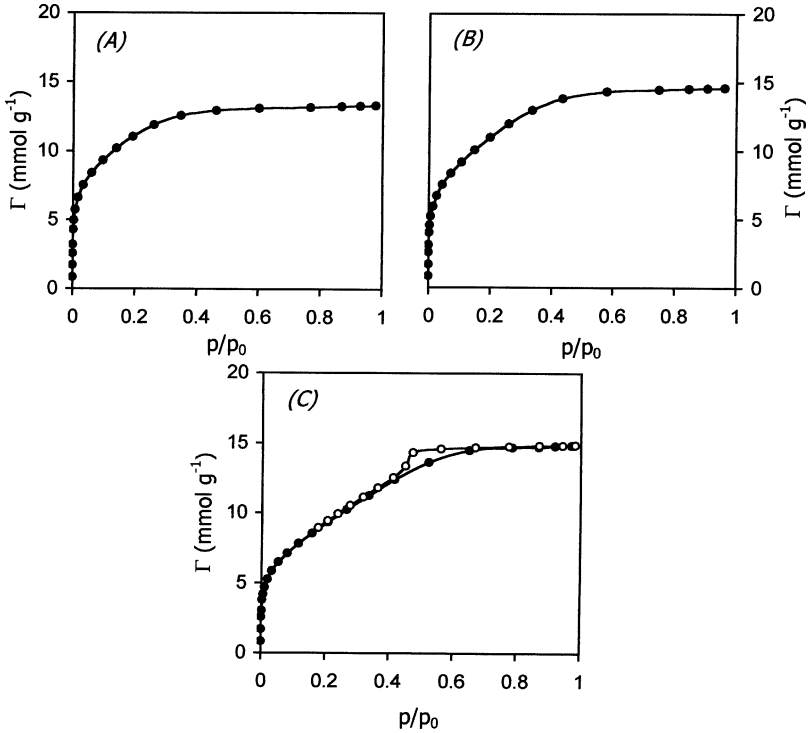

Figure 1. Adsorption−desorption isotherms of nitrogen at 77 K onto calcined aluminosilicate monoliths prepared with various Si:Al molar ratios: (A) SiAl20, (B) SiAl10, and (C) SiAl5.

K on samples previously outgassed overnight down to 10^{-3} Torr at 493 K. BET plots were constructed below a relative pressure of 0.2 from the adsorption branches. These lines were subsequently used to evaluate the BET specific surface area, S_{BET}, taking a cross-sectional area of 0.162 nm^2 per nitrogen molecule. The improved MP method,[27] based on analysis of the adsorption branch, was used to determine parameters of the "average" pore network, that is, the mesopore and micropore volumes, V_{mes} and V_{mic}, and the mesopore diameter, d_p. The number of surface acid sites in the various samples was evaluated by two-cycle adsorption of ammonia at 373 K using a Micromeritics ASAP 2010 apparatus. At the end of the first adsorption cycle, the sample was outgassed under vacuum at 373 K for 30 min and a second adsorption cycle was performed at the same temperature. The linear segments of each adsorption isotherm at higher pressures were suitably extrapolated to zero pressure. The difference between the adsorption values corresponding to the two intersection points was taken as the estimate of the total number of acidic sites in the sample.[28] Similar adsorption procedures were employed to study the individual adsorption of propane and propene at 298 K under batch conditions. Prior to adsorption experiments, the samples were outgassed overnight at 423 K.

Results and Discussion

Characterization of Monolithic Samples. The calcined silica or aluminosilicate monoliths studied here are optically transparent and crack-free cylinders of ca. 1.5 mm in diameter and their length ranges between 4 and 5 mm (see †Supporting Information). The moulded cylindrical aluminosilicates possess small mesopores, as evidenced by the nitrogen adsorption−desorption isotherms shown in Figure 1. The adsorption curves fall somewhere between type I and type IV isotherms. For SiAl20 and SiAl10, the adsorption phenomenon is completely reversible (so the desorption branches are not shown). In the case of a sample rich in aluminum (SiAl5), a small hysteresis loop can be seen at moderate relative pressures. A gradual increase in the amount of N_2 adsorbed at low and moderate pressures means that the porosity is to some extent heterogeneous. The values of the BET specific surface area, S_{BET}, and of the "average" pore structure parameters are collected in Table 1. The purely siliceous sample is almost microporous with a mean pore diameter of 2.1 nm and a small pore volume. Clearly, introducing aluminum in the silica matrix causes the mean pore diameter to increase. The analysis of the adsorption isotherms in Figure 1 indicates that less ordered porous structures are obtained, and the use of polydisperse industrial surfactants may be responsible for such disorder.[27] Fundamentally, some heterogeneity in the pore size distribution cannot be considered as a great disadvantage in a separation technology based on the π-complexation mechanism. On the contrary, the application of cheap template sources is an important argument for cost reduction. The XRD patterns of the calcined samples prepared using three different Si:Al molar ratios are shown in Figure 2. Only a single first-order scattering peak is observed at very small angles and its intensity decreases with increasing Al content. It seems that the introduction of aluminum into the framework of monolithic silica contributes to the overall heterogeneity of the internal nanostructure.

Table 1. Specific Surface Area, S_{BET}, Mesopore Volume, V_{mes}, Mean Pore Diameter, d_p, and Number of Acid Sites, n_a, for the Monolithic Aluminosilicate Samples Prepared with Various Si:Al Molar Ratios

sample	S_{BET} ($m^2\ g^{-1}$)	V_{mes} ($cm^3\ g^{-1}$)	d_p (nm)	n_a ($\mu mol\ m^{-2}$)
SiO_2	746	0.28	2.1	0.13
SiAl20	911	0.38	2.4	0.48
SiAl10	915	0.44	2.9	0.52
SiAl5	770	0.46	3.6	0.77

(28) Zajac, J.; Dutartre, R.; Jones, D. J.; Rozière, J. *Thermochim. Acta* **2001**, *379*, 123.

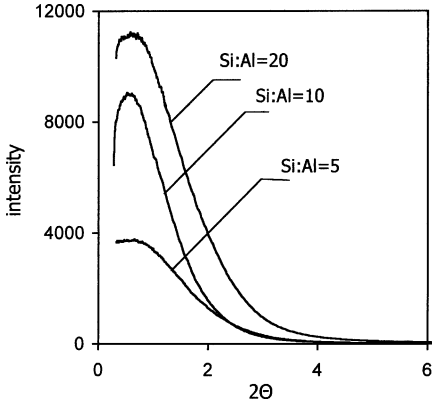

Figure 2. Powder X-ray diffraction patterns for calcined aluminosilicate samples prepared with various Si:Al molar ratios.

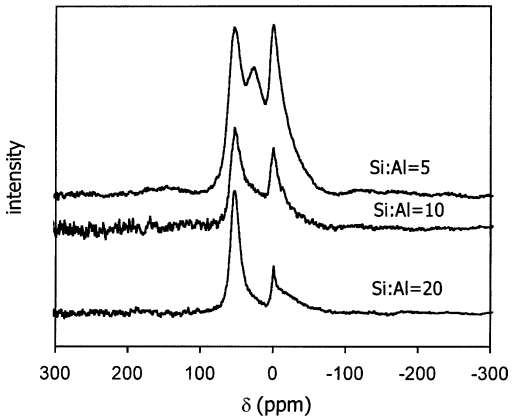

Figure 3. ^{27}Al MAS NMR spectra of calcined aluminosilicate monoliths prepared with various Si:Al molar ratios.

The framework aluminum plays a very important role in conferring certain properties of silica-based materials, by enhancing their surface acidity, ion-exchange capacity, and thermal/mechanical stability.[27] For the samples studied in the present paper, the total number of acid sites, as measured by the two-cycle adsorption of ammonia at 373 K, is given in Table 1. As expected, the surface density of acid sites increases with increasing aluminum content. The degree of aluminum incorporation into the framework can be assessed from the ^{27}Al MAS NMR spectra presented in Figure 3. The NMR spectra of the calcined aluminosilicates show relatively sharp resonance at 52 ppm due to tetrahedrally coordinated Al. The appearance of a second signal at $\delta \approx 0$ ppm indicates that extraframework Al is also present. The relative intensity of this second signal increases with increasing Al content. In the case of the sample prepared with a Si:Al ratio of 5, a quite strong resonance at ca. 30 ppm may be ascribed to 5-coordinated Al.[29] The presence of extraframework Al in the monoliths rich in aluminum and the simultaneous broadening of their pores should be taken into consideration when optimizing the materials for selective propene−propane separation.

The shaped aluminosilicates with a Si:Al ratio of 20, 10, and 5 were subsequently used as supports for copper and silver centers by ion exchange. The derivatization

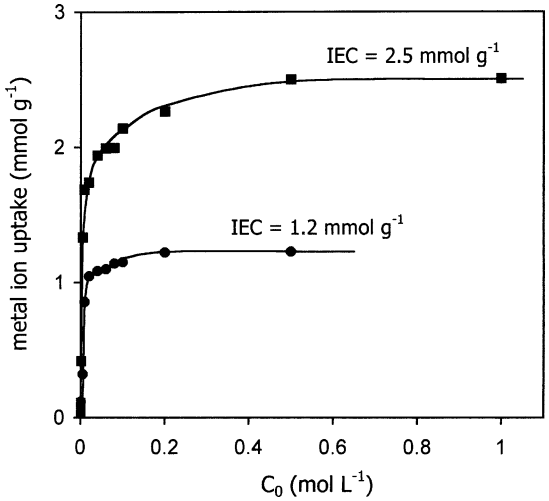

Figure 4. Cu^{2+} (circles) and Ag^+ (squares) uptake by SiAl20 from aqueous solutions of Cu(II) or Ag(I) nitrate plotted against the initial solution concentration, C_0.

Table 2. Ion-Exchange Capacity, IEC, and Metal Ion Loading Quantity, of Shaped Aluminosilicate Materials

	sample		
parameter	SiAl20	SiAl10	SiAl5
Cu calculated IEC (mmol g^{-1})	0.4	0.8	1.7
Cu experimental IEC (mmol g^{-1})	1.2	1.9	0.7
Cu^{2+} content in the solid sample (wt %)	7.2	10.7	4.3
Ag calculated IEC (mmol g^{-1})	0.8	1.7	3.3
Ag experimental IEC (mmol g^{-1})	2.3	2.5	2.9
Ag^+ content in the solid sample (wt %)	19.6	21.3	24.2

procedure was carried out from concentrated solutions of Cu and Ag so as to attain a high degree of metal incorporation.

The ion-exchange capacity for both metal ions was determined by measuring the uptake of Cu^{2+} and Ag^+ by the pristine samples from aqueous solutions of $Cu(NO_3)_2$ and $AgNO_3$ at different salt concentrations. Figure 4 presents two ion-exchange curves for a selected sample. The uptake of metal ions by SiAl20 first increases with increasing concentration of $Cu(NO_3)_2$ or $AgNO_3$ solution and then it levels off above $C_0 = 0.2$ mol L^{-1} (Cu) or $C_0 = 0.5$ mol L^{-1} (Ag). The uptake values in the plateau exchange region provide estimates of the ion-exchange capacity, IEC, per unit mass of SiAl20 for both metal ions. The experimental IEC values determined in the same manner for other shaped aluminosilicates are collected in Table 2. They are compared with the IEC estimates calculated based on the overall Si:Al ratio in each pristine sample and assuming that only "permanent" negative charge due to isomorphous replacement is responsible for exchange capacity of aluminosilicate samples. The calculated IEC values in Table 2 seem underestimated. This is mainly because the role of the pH-dependent charge (chemisorbed OH groups) has been neglected, as being difficult to quantify. According to the results reported in the literature,[30−32] the actual density of surface hydroxyls depends not only on the amount of aluminum incorporated into the framework but also on the sample porosity.[32]

(29) Zhao, H.; Hiragushi, K.; Mizota, Y. J. *Non-Cryst. Solids* **2002**, *311*, 199.

(30) Whalen, J. W. *J. Phys. Chem.* **1967**, *71*, 1557.
(31) Peri, J. B. *J. Phys. Chem.* **1965**, *69*, 211.
(32) Meziani, M. J.; Zajac, J.; Douillard, J.-M.; Jones, D. J.; Partyka, S.; Rozière, J. *J. Colloid Interface Sci.* **2001**, *233*, 219.

Table 3. Pore Structure Parameters of Cu-Ion-Exchanged Aluminosilicate Monoliths

sample	Cu content (wt %)	S_{BET} ($m^2\ g^{-1}$)	V_{mes} ($cm^3\ g^{-1}$)	d_p (nm)	V_{mic} ($cm^3\ g^{-1}$)
SiAl20Cu	7.2	384	0.25	2.9	
SiAl10Cu	10.7	533	0.27	3.4	0.05
SiAl5Cu	4.3	509	0.32	4.4	0.05

Table 4. Pore Structure Parameters of Ag-Ion-Exchanged Aluminosilicate Monoliths

sample	Ag content (wt %)	S_{BET} ($m^2\ g^{-1}$)	V_{mes} ($cm^3\ g^{-1}$)	d_p (nm)	V_{mic} ($cm^3\ g^{-1}$)
SiAl20Ag	19.6	258	0.25	3.9	
SiAl10Ag	21.3	347	0.26	3.6	0.01
SiAl5Ag	24.2	470	0.30	4.3	0.04

It should also be noted that only silanol groups may take part in ion exchange under neutral pH conditions of the experiment.

With the cylindrically shaped aluminosilicates studied here, the effectiveness of ion exchange is dependent on both the metal nature and the Si:Al ratio. In the case of SiAl20, the IEC value for Cu(II) is exactly half that obtained for Ag(I), which indicates that the number of exchangeable sites in this sample is the same for both ions. In other samples, the exchangeable sites are more heterogeneous, and in the case of SiAl10, they show more affinity for Cu(II) than for Ag(I), whereas the opposite trend is reported on SiAl5.

The experimentally measured IEC values were further used to calculate the maximum metal content in a given sample, as the ratio between the mass of the incorporated metal and the overall mass of the derivatized sample. The results are given in Table 2.

For the purpose of the present work, the shaped aluminosilicates have been derivatized by ion exchange from 0.5 mol L^{-1} $Cu(NO_3)_2$ and 1 mol L^{-1} $AgNO_3$ aqueous solutions. Therefore, the metal loading by each sample corresponds (within the range of experimental error) to the appropriate metal content reported in Table 2. Note that the average relative uncertainty in determining the experimental IEC parameters, associated with AAS analysis and manual operations accompanying the dissolution of solid samples and the preparation of solutions, was evaluated for about 10%. Such derivatized samples are characterized by the best selectivity performance toward propene against propane and this performance is lowered when decreasing the overall metal content.

The BET specific surface area and the pore structure parameters for the copper- and silver-derivatized samples are given in Tables 3 and 4. Generally, the derivatized materials possess larger pores and lower specific surface areas than the pristine aluminosilicate cylinders. Similar trends have been observed for samples maintained in aqueous solution for 24 h. The increase in the mean pore size may thus be attributed to hydrolytically induced changes in the adsorbent porosity.

Adsorption of Propene and Propane onto Derivatized Monoliths. Adsorption of propane and propene was studied under static conditions at room temperature. The Cu(II)-exchanged samples cannot be considered as the most relevant for selective separation of propene and propane. However, ion exchange with Cu(I) cannot be carried out in an aqueous medium, and SiAl20Cu was additionally modified by a partial reduction of Cu(II) to Cu(I). This sample was first outgassed and then treated with hydrogen at 450 K, this temperature having been previously determined from hydrogen TPR. This monolith is referred to hereafter as $SiAl20Cu_{red}$.

The equilibrium isotherms of individual adsorption of propane and propene are shown in Figures 5 and 6. The adsorption curves are of the Freundlich type, namely, $\Gamma = kp^n$ where Γ is the amount adsorbed at equilibrium pressure p and k and n are Freundlich constants. The best-fit values of parameter n for both gases reported in Table 5 are smaller than unity, thereby revealing the energetic heterogeneity of the solid surface. In the case of propene, the values of n are

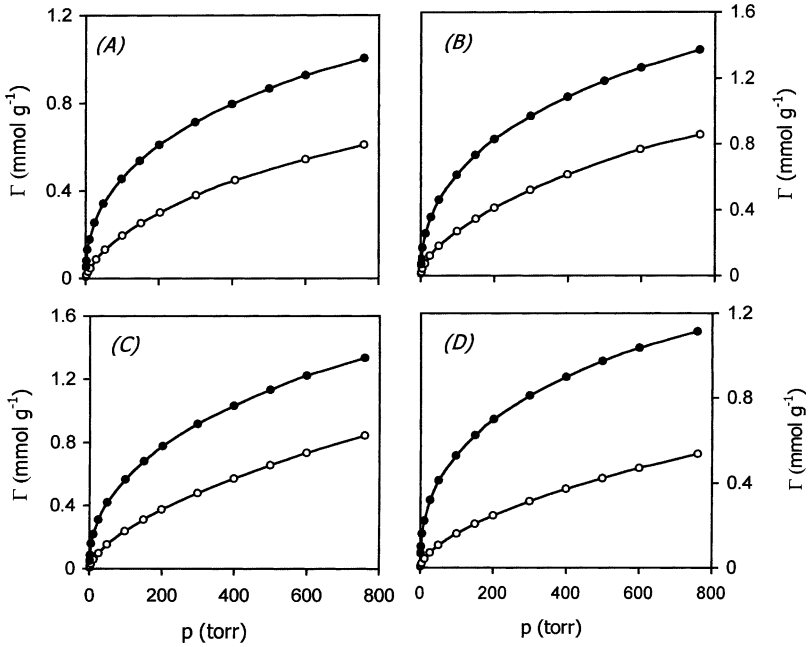

Figure 5. Individual adsorption isotherms of propene (solid circles) and propane (open circles) on copper-functionalized cylinders prepared with various Si:Al molar ratios: (A) SiAl20Cu, (B) SiAl10Cu, (C) SiAl5Cu, and (D) $SiAl20Cu_{red}$.

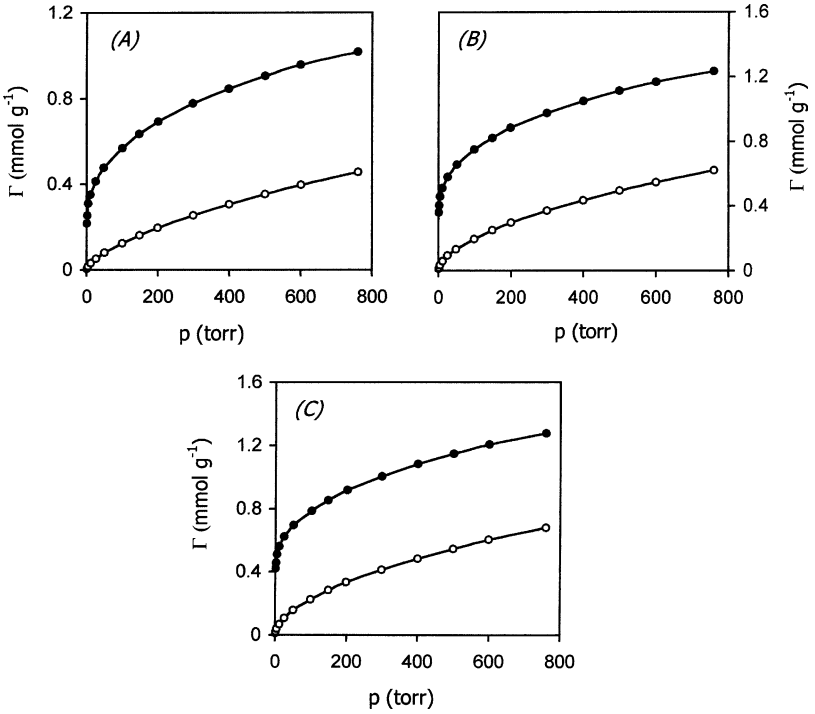

Figure 6. Individual adsorption isotherms of propene (solid circles) and propane (open circles) on silver-functionalized cylinders prepared with various Si:Al molar ratios: (A) SiAl20Ag, (B) SiAl10Ag, and (C) SiAl5Ag.

Table 5. Best-Fit Value of the Exponent Freundlich Constant, Surface Density of Metal Ion Sites, and Adsorption Capacity Ratios for Propene (2)/Propane (1) at Two Selected Pressures for the Various Ion-Exchanged Monoliths

	Freundlich constant n		surface density of M^{n+} sites	Γ_2/Γ_1 at a given p	
sample	propene (2)	propane (1)	(μmol m^{-2})	40 Torr	760 Torr
SiAl20Cu	0.43	0.67	3.1	3.0	1.5
SiAl10Cu	0.44	0.63	3.6	2.7	1.5
SiAl5Cu	0.47	0.68	1.4	2.9	1.6
$SiAl20Cu_{red}$	0.41	0.67		4.3	2.0
SiAl20Ag	0.23	0.70	8.9	7.8	1.9
SiAl10Ag	0.18	0.61	7.2	6.1	1.8
SiAl5Ag	0.17	0.60	6.2	5.7	1.6

much smaller than 1, which means that interactions of this gas with the surface-active sites are particularly heterogeneous. Here, the initial portions of the corresponding isotherms are quasi-vertical, and chemisorption clearly contributes, while the shape of adsorption curves for propane indicates the adsorption phenomenon to be predominantly physical in character.

For all samples studied, the amount of adsorbed propene at a given equilibrium pressure is much greater than that of propane. The effect is particularly marked at low equilibrium pressures. The overall adsorption capacity for propene at 760 Torr ranges between 1.0 and 1.4 mmol g^{-1}. The individual adsorption ratio for propene over propane decreases with increasing pressure, the differences among the samples being pronounced only at low pressures. Table 5 presents the ratio values for two selected pressures of 40 and 760 Torr, together with the surface density of metal ionic sites calculated by dividing the appropriate IEC value by the BET specific surface area. At first sight the adsorption capacity ratio at 40 Torr increases with increasing surface density of ionic sites, although this dependence is not so regular for the samples containing Cu. Ag-functionalized monoliths exhibit higher adsorption affinity for propene against propane than their Cu homologues. SiAl20Ag is characterized by the highest capacity ratio for propene/propane, which is equal to 7.8 at 40 Torr. In the series of Cu-functionalized samples, $SiAl20Cu_{red}$ has an adsorption capacity ratio better than those of all the Cu(II)-exchanged monoliths. Here, adsorption of propene is favored over propane by a ratio of 4.3 at 40 Torr. The enhanced capacity ratio for propene/propane of these two types of sample supports the hypothesis that monovalent cationic sites, Cu^+ and Ag^+, are more appropriate for the selective adsorption.

Adsorption Selectivity of the Derivatized Monoliths. The higher adsorption affinity of Cu- and Ag-derivatized aluminosilicate cylinders toward propene compared to propane is expected to be useful for selective separation of binary gas mixtures. Based on the individual adsorption isotherms of propane and propene under static conditions, the equilibrium selectivity of propene toward propane was calculated from the compositions of the adsorbed phase and the binary gas mixture.[15] If one assumes that propane and propene behave as perfect gases and that their adsorption on active surface sites is additive and depends only on the partial pressure of a given component in the gas mixture (propane, component 1; propene, component 2), the ideal selectivity coefficient S_{21} may be calculated as a function of the mole fraction of propene in the gas mixture using the following expressions,

$$S_{21} = \frac{\Gamma_2 \cdot (1 - X_2)}{\Gamma_1 \cdot X_2} \text{ and } X_2 = \frac{p_2}{760}$$

where p_2 is the equilibrium pressure (in Torr) of propene considered equal to its partial pressure in the binary mixture and Γ_1 and Γ_2 are the amounts adsorbed of propane and propene, respectively. A selectivity coef-

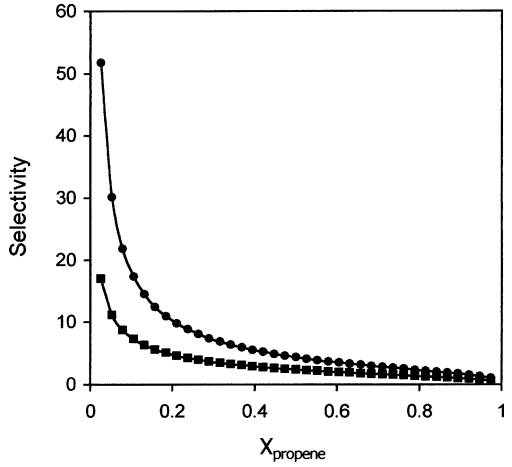

Figure 7. Equilibrium selectivity coefficient plotted against the mole fraction of propene in the propane−propene gaseous mixture for two selected aluminosilicate cylinders: SiAl20Ag (circles) and SiAl20Cu$_{red}$ (squares).

Table 6. Ideal Selectivity for Aluminosilicate Cylinders Derivatized with Cu and Ag at Different Mole Fractions of Propene in the Bulk Mixture

	equilibrium selectivity at a given $X_{propene}$			
sample	0.05	0.3	0.5	0.7
SiAl20Cu	11.7	2.5	1.8	1.2
SiAl10Cu	11.6	2.5	1.7	1.2
SiAl5Cu	10.8	2.6	1.8	1.3
SiAl20Cu$_{red}$	17.0	3.5	2.4	1.6
SiAl20Ag	51.8	6.9	4.4	2.8
SiAl10Ag	33.8	3.9	2.4	1.4
SiAl5Ag	33.4	3.6	2.2	1.3

ficient equal to unity means that the compositions of both phases are identical and the adsorption phenomenon is unselective. The propene/propane selectivity so determined is plotted against the propene mole fraction X_2 in Figure 7 for the best sample within each category. As for the adsorption capacity ratio, the selectivity coefficient decreases with increasing mole fraction of propene in the mixture. Both samples appear very efficient for selective adsorption of propene from gas mixtures containing small amounts of this component. For small equilibrium pressures of propene, adsorption is probably restricted to chemisorption and the amounts adsorbed are quite high. Since propane can only be physisorbed, it cannot compete efficiently with the alkene for the most active surface sites. In consequence, the selectivity coefficient attains high values. When the gas mixture becomes richer in propene, the adsorption of both components is dominated by the physisorption contribution and the overall selectivity diminishes. This also means that only a small fraction of surface sites is active enough for propene to chemisorb on the surface.

The values of the ideal selectivity coefficient for four selected gas compositions are collected in Table 6 and provide the basis on which different samples may be compared. The Ag-derivatized monoliths are characterized by much higher selectivity than those containing Cu, irrespective of the composition of the gas mixture. SiAl20Ag has the biggest selectivity coefficient, which can attain a value of ca. 52 at small mole fractions of propene in the binary mixture. The two other samples show almost the same X_2-dependence of S_{21} and there is no difference between their selectivities. The three monoliths derivatized with Cu(II) have practically the same selectivity behavior. The performance of SiAlCu$_{red}$ is much better because its selectivity at $X_2 = 0.05$ is almost doubled. This confirms that monovalent Cu species provide more reactive sites for selective propene adsorption against propane. No clear trends in S_{21} with the Si:Al ratio or the mean pore size can be deduced from the results reported in Table 6, and in fact the amount of Al in the framework even seems to have little if any effect on propene/propane selectivity.

Derivatized Aluminosilicate Monoliths and Prospects for Their Applications. Zeolites such as 13X, MFI, or A[33,34] and other microporous materials, such as carbon molecular sieves,[35] are common sorbents for gas separations based on pressure/vacuum swing adsorption (PSA-VSA) processes, where molecular size and/or shape selectivity effects can be exploited either kinetically or in equilibrium mode. However, there are several problems preventing the commercial use of microporous materials in PSA alkene−alkane separation processes. As zeolite cavities or micropores are of molecular dimensions, alkene sorption in such crystals at ambient temperatures is characterized by very low intracrystalline diffusivity and large overall mass-transfer resistance, leading to incomplete solid regeneration during the blowdown steps[36] and/or impractical large cycle times[24] when a vacuum swing adsorption (VSA) process is implemented.[37] As a consequence, higher process temperatures (100−200 °C) are often employed, but even though the problems of equilibrium irreversibility and mass-transfer resistances are diminished, selectivity and capacity are simultaneously reduced and coke deposition over the solid sorbent or alkene polymerization can occur.[38,39]

On the other hand, a sorption separation procedure calls for integration of the adsorbent and the adsorber. The most obvious adsorber contains a fixed adsorbent bed, which involves a stacking of porous adsorbent bodies. To limit the pressure drop over the adsorbent bed, the adsorbent bodies must be of macroscopic dimensions and, consequently, powdered materials cannot be directly used. The industrial formulation of adsorbents is a major technological challenge, requiring pressing or extruding the pristine powdered material into a mechanically stable macroporous form suitable for industrial use. Such treatment may cause damage to the pore structure, compromising the surface area and pore volume. Additionally, extra "intercrystalline" mass-transfer resistances are created and, in many cases, the process kinetics is controlled by the pellet or extrudate size.[40] The DLCT method used in the present work allows direct preparation of shaped homogeneous

(33) Grande, C. A.; Gigola, C.; Rodrigues, A. E. *Ind. Eng. Chem. Res.* **2002**, *41*, 85.
(34) Masuda, T.; Okubo, Y.; Mukai, S. R.; Kawase, M.; Hashimoto, K.; Shichi, A.; Satsuma, A.; Hattori, T.; Kiyozumi, Y. *Chem. Eng. Sci.* **2001**, *56*, 889.
(35) Grande, C. A.; Silva, V. M. T. M.; Gigola, C.; Rodrigues, A. E. *Carbon* **2003**, *41*, 2533.
(36) Da Silva, F. A.; Rodrigues, A. E. *Ind. Eng. Chem. Res.* **1999**, *38*, 2051.
(37) Sikavitsas, V. I.; Yang, R.; Burns, M.; Langenmayr, E. *Ind. Eng. Chem. Res.* **1995**, *34*, 2873.
(38) Boucheffa, Y.; Thomazeau, C.; Cartraud, P.; Magnoux, P.; Guisnet, M.; Jullian, S. *Ind. Eng. Chem. Res.* **1997**, *36*, 3198.
(39) Järvelin, H.; Fair, J. R. *Ind. Eng. Chem. Res.* **1993**, *32*, 2201.
(40) Kärger, J.; Ruthven, D. M. *Diffusion in Zeolites*; John Wiley & Sons: New York, 1992; p 104.

monoliths that present high specific surface area, controllable mesopore sizes, and ion-exchange capacity conferred by the presence of aluminum. Their interfacial properties are similar to those presented by powdered aluminosilicates of the MCM-41 type.[41−43] The possibility of moulding macroscopic-in-size objects is an attractive alternative. The selective adsorption properties of monolithic aluminosilicates derivatized with Cu and Ag, as well as the improved accessibility of active centers, make them adequate for uses in PSA processes, especially for low propene contents in the gas mixture.

The selective adsorption properties of derivatized aluminosilicate monoliths have been predicted from the individual adsorption of propene and propane on the basis of their ideal mixing behavior both in the adsorbed phase and in the bulk mixture. At present, one can only speculate on the evolution of the selectivity mechanism from real gas mixtures and further studies are necessary in order to make use of functionalized materials formulated to act as membranes. The preparation of moulded cylindrical aluminosilicates may be considered as a first step toward membrane development, which can involve either the preparation of self-supported aluminosilicate hollow fibers or the deposition of thin layers on ceramic monoliths of a low surface area by dip-coating or spin-coating and subsequent loading with the appropriate transition metal.

Conclusion

Mesoporous aluminosilicate cylinders can be easily moulded via the direct liquid crystal templating pathway and using nonionic surfactants as structure-directing agents. Further functionalization with Cu and Ag following the ion-exchange procedure provides monoliths possessing good selectivity for gaseous propene/propane mixtures. The high adsorption selectivity of propene over propane, especially at low alkene concentrations, is attributed to chemisorption of the unsaturated hydrocarbon molecules on surface sites due to the presence of the transition metal. The nature and the number of surface metal sites are likely to be crucial for selective adsorption of propene against propane.

Acknowledgment. Financial support from the European Growth Contract No. G5RD-CT-2001-00544 is acknowledged with thanks.

Supporting Information Available: Photograph of moulded cylindrical aluminosilicates (PDF). This material is available free of charge via the Internet at http://pubs.acs.org.

CM040051L

(41) Meziani, M.; Zajac, J.; Jones, D. J.; Rozière, J.; Partyka, S. *Langmuir* **1997**, *13*, 5409.

(42) Luan, Zh.; Cheng, C.-F.; Zhou, W.; Klinowski, J. *J. Phys. Chem.* **1995**, *99*, 1018.

(43) Janicke, M.; Kumar, D.; Stucky, G. D.; Chmelka, B. F. In *Zeolites and Related Microporous Materials: State of the Art 1994*; Weitkamp, J., Karge, H. G., Pfeifer, H., Holderich, W., Eds.; Studies in Surface Science and Catalysis, Vol. 84; Elsevier: Amsterdam, 1994; p 243.